

Gravity derived crustal thickness model of Botswana: Its implication for the Mw 6.5 April 3, 2017, Botswana earthquake

Chikondi Chisenga, Mark Van der Meijde, Yan Jianguo, Islam Fadel, Estella A. Atekwana, Rebekka Steffen, Calistus Ramotoroko

PII: S0040-1951(20)30162-1

DOI: <https://doi.org/10.1016/j.tecto.2020.228479>

Reference: TECTO 228479

To appear in: *Tectonophysics*

Received date: 22 July 2019

Revised date: 15 March 2020

Accepted date: 17 May 2020

Please cite this article as: C. Chisenga, M. Van der Meijde, Y. Jianguo, et al., Gravity derived crustal thickness model of Botswana: Its implication for the Mw 6.5 April 3, 2017, Botswana earthquake, *Tectonophysics* (2020), <https://doi.org/10.1016/j.tecto.2020.228479>

This is a PDF file of an article that has undergone enhancements after acceptance, such as the addition of a cover page and metadata, and formatting for readability, but it is not yet the definitive version of record. This version will undergo additional copyediting, typesetting and review before it is published in its final form, but we are providing this version to give early visibility of the article. Please note that, during the production process, errors may be discovered which could affect the content, and all legal disclaimers that apply to the journal pertain.

**Gravity Derived Crustal Thickness Model of Botswana: Its implication for the  $M_w$  6.5****April 3, 2017, Botswana Earthquake**

Chikondi Chisenga<sup>1,2</sup>, Mark Van der Meijde<sup>3</sup>, Yan Jianguo<sup>1</sup>, Islam Fadel<sup>3</sup>, Estella A. Atekwana<sup>4</sup>, Rebekka Steffen<sup>5</sup>, Calistus Ramotoroko<sup>6</sup>

<sup>1</sup>State Key Laboratory of Information Engineering in Surveying, Mapping and Remote Sensing (LIESMARS), Wuhan University, Box 129, Luoyu Road, Wuhan, China.

<sup>2</sup>Department of Earth Sciences, Ndata School of Climate and Earth Sciences, Malawi University of Science and Technology, P.O. Box 5196, Limbe, Malawi

<sup>3</sup>University of Twente, Faculty for Geo-information Science and Earth Observation (ITC), P.O. Box 6, 7500 AA Enschede, The Netherlands

<sup>4</sup>Department of Earth Sciences, College of Earth, Ocean, and Environment, University of Delaware, Newark, Delaware, 19716 USA

<sup>5</sup>Lantmäteriet, Lantmäterigatan 2C, 80182 Göteborg, Sweden

<sup>6</sup>Department of Physics and Astronomy, Botswana International University of Science and Technology, Palapye, Botswana

**Abstract**

Botswana experienced a  $M_w$  6.5 earthquake on 3<sup>rd</sup> April, 2017, the second largest earthquake event in Botswana's recorded history. This earthquake occurred within the Limpopo-Shashe Belt, ~350 km southeast of the seismically active Okavango Rift Zone. The region has no historical record of large magnitude earthquakes or active faults. The occurrence of this earthquake was unexpected and underscores our limited understanding of the crustal configuration of Botswana and highlights that neotectonic activity is not only confined to the Okavango Rift Zone. To address this knowledge gap, we applied a regularized inversion algorithm to the Bouguer gravity data to construct a high-resolution crustal thickness map of Botswana. The produced crustal thickness map shows a thinner crust (35-40 km) underlying the Okavango Rift Zone and sedimentary basins, whereas thicker crust (41-46 km) underlies the

cratonic regions and orogenic belts. Our results also show localized zone of relatively thinner crust (~40 km), one of which is located along the edge of the Kaapvaal Craton within the M<sub>w</sub> 6.5 Botswana earthquake region. Based on our result, we propose a mechanism of the Botswana Earthquake that integrates crustal thickness information with elevated heat flow as the result of the thermal fluid from East African Rift System, and extensional forces predicted by the local stress regime. The epicentral region is therefore suggested to be a possible area of tectonic reactivation, which is caused by multiple factors that could lead to future intraplate earthquakes in this region.

**Keywords:** Moiyabana Epicentral Region; Intraplate earthquake, gravity inversion; crustal thickness; Botswana

## 1. Introduction

Most large and deep earthquakes occur in active tectonic and deformational zones along plate boundaries, where tectonic stress is released as earthquakes. Nevertheless, large intraplate earthquakes, with moment magnitudes above M<sub>w</sub> 6.0, rarely occur in continental interiors. The vast majority of intraplate earthquakes that occur far from known plate boundaries are associated with rifting and extension regions (Craig et al., 2011), and a few have been recorded in stable continental regions (e.g., Talwani, 2014; Calais et al., 2016). Factors controlling such intraplate earthquakes include a gradient in lithospheric thickness and the presence of weak zones at crustal scale boundaries, especially cratonic edges, formed as a result of crustal blocks amalgamation during continental buildup (e.g., Mooney et al., 2012; Sloan et al., 2011; Tesauro et al., 2015). These crustal boundaries remain weak zones and can be reactivated and trigger earthquakes. Examples of large intraplate earthquakes include the 1811-1812 New Madrid event in the Mississippi Valley of the central U.S, the 1988 Tennant Creek earthquake in Australia, and in recent years, the 2001 earthquakes in the ancient Kachchh rift basin in Western India (Calais et al., 2016). Nevertheless, the controlling mechanism for such types of earthquakes is difficult to explain, especially when not associated with neo-tectonic activity.

On April 3<sup>rd</sup>, 2017, a large intraplate earthquake with a magnitude of M<sub>w</sub> 6.5 occurred in eastern Botswana in the area of Moiyabana, historically recorded as the second largest earthquake since

1952 (Midzi et al., 2018). The earthquake occurred within the Southern Marginal Zone of the Limpopo-Shashe Belt, an Archean belt that represents a collisional zone between the Kaapvaal and the Zimbabwe Cratons. This area is about 350 km southeast of the seismically active Okavango Rift Zone and shows no sign of neotectonic activities as well as no historical records of large magnitude earthquakes (Kolawole et al., 2017; Midzi et al., 2018). The earthquake was a normal faulting event that reactivated an old thrust sheet in a weak zone with a contrast in material properties (Kolawole et al., 2017; Midzi et al., 2018; Gardonio et al., 2018; Materna et al., 2019). The causative fault for the Botswana earthquake revealed a 1.8 m displacement, striking in the NW direction, dipping to the northeast (Kolawole et al., 2017), which is consistent with the predicted local stress regime (e.g., Stamps et al., 2010; Kolawole et al., 2017). The rupture occurred at a depth of 21–24 km (Kolawole et al., 2017), while other studies estimated a depth of 21 km (Albano et al., 2017) and 29 km (Gardonio et al., 2018). Both Kolawole et al. (2017) and Albano et al. (2017) suggested that extensional forces triggered the earthquake and reactivated crustal-scale Precambrian thrust sheets within the Limpopo-Shashe Belt. However, Gardonio et al. (2018) attributed the event to the episodic fluid release from the upper mantle that reactivated the elastically stressed weak zone. Such a weak zone was resolved in the lower crust and upper mantle beneath the Moiyabana Epicentral Region (Moorkamp et al., 2019; Materna et al., 2019). Nevertheless, the source of the fluid release in the upper mantle beneath the Moiyabana Epicentral Region is still unclear (Moorkamp et al., 2019). Fadel et al., (2020) however, suggested that the source of fluid in the Moiyabana Epicentral Region is the East African Rift System, based on the 3D crustal and upper mantle shear wave velocity structure of Botswana. They suggested that the fluids originated at a depth of ~150 km at the northeastern tip of Botswana and migrate to the edge of the Kaapvaal Craton. Thus, the mechanism for this earthquake remains debatable due to multiple theories, underscoring the need for more detailed knowledge on the crustal architecture beneath the Moiyabana Epicentral Region.

Despite decades of exploration efforts related to mining and the installation of more seismic stations since 2000 (e.g., Nyblade and Dirks, 2006; Simon et al., 2012; Gao et al., 2013; Fadel et al., 2018), knowledge on the deep crustal structure of Botswana remains limited. Existing crustal structure models derived from seismic stations spacing ~25 to 100 km (e.g., Fadel et al., 2018; Kachingwe et al., 2015; Yu et al., 2015) do not provide sufficient details to resolve the finer

crustal structure beneath the Moiyabana Epicentral Region. Here we take advantage of the existing high resolution gravity data with a uniform grid of ~7.5 km that exists over the entire country to estimate crustal structure beneath Botswana and the Moiyabana Epicentral Region. Gravity derived crustal thickness models can provide more details on the crustal structure compared to seismic estimates in regions where the distribution of seismic stations is sparse (van der Meijde et al., 2015). We applied a regularizing inversion algorithm to the Bouguer gravity data (Uieda & Barbosa, 2017). The resolved crustal thickness model is then validated with seismic crustal thickness estimates from seismic receiver function and *H-K* stacking analyses (Yousouf et al., 2014; Yu et al., 2015; Fadel et al., 2018). We examine the gravity derived crustal structure of Botswana to understand the crustal architecture underneath Botswana and the possible causes of the  $M_w$  6.5 earthquake. Finally, we propose a mechanism for this earthquake based on the integration of the crustal structure information with previously obtained information on the local stress regime, and the fault system, which could have led to the occurrence of the Botswana Earthquake.

## 2. Tectonic setting

The Botswana crust is made up of two major cratonic blocks, the Kalahari and Congo Cratons that are surrounded by orogenic mobile belts (Figure 1; Begg et al., 2009; and references therein). The Kalahari Craton consists of the amalgamation of the Kaapvaal and Zimbabwe Cratons sutured at the Neo-Archean Limpopo-Shashe Belt (Clifford, 1970). The Zimbabwe Craton comprises different tectonic and geological terranes that formed between 3.6 and 2.4 Ga. The Kaapvaal Craton was formed by the amalgamation of several geological units, mostly consisting of granitoids with gneisses and narrow greenstone belts, between 3.7 and 2.7 Ga (Begg et al., 2009). The adjoining Neo-Archean Limpopo-Shashe Belt is a WNW-ESE trending belt comprised of high-grade metamorphic rocks and formed between 2.7 and 2.6 Ga during the collision of the Zimbabwe Craton and the Kaapvaal Craton (Key and Ayres, 2000; Ranganai et al., 2002). In Botswana, the boundary between the Limpopo-Shashe Belt and the Zimbabwe Craton is placed on the Shashe thrust zone (Ranganai et al., 2002). The Limpopo-Shashe Belt is divided into the Northern Marginal Zone, the Central Zone, and the Southern Marginal Zone, based on the lithological and structural similarities (Figure 1; Ranganai et al., 2002).

The Kalahari Craton is surrounded by Proterozoic mobile belts and mafic complexes, some of which intruded and affected this stable cratonic crustal block (Begg et al., 2009; and references therein). For example, the Southern Marginal Zone was intruded and affected by the Mahalapye Granite Complex during the uplifting and thinning in the Limpopo-Shashe belt (McCourt et al., 1995) and the Central Zone was affected by a sub-vertical crustal lineament forming the Palala shear zone (Schaller, 1999). The Kalahari Suture Zone, a Paleo-Proterozoic thrust zone, is located in the western and northern margins of the Kalahari Craton. The Kalahari Suture Zone played a major role in the formation of the Kheis-Okwa-Xade-Magondi Belts and also separates the Kalahari Craton from the Damara-Ghanzi-Chobe Proterozoic Belt (e.g., Reeves & Hutchins, 1982). The Kalahari Suture Zone consists of the Kalahari Line, which extends from South Africa into southern Botswana along the Kheis-Okwa Belt, and the Makgadikgadi Line, which is the northern edge of the Kaapvaal Craton extending northeastwards to the Magondi Belt (Figure 1).

The Damara and the Ghanzi-Chobe Proterozoic Belts separate the Congo Craton and the Kalahari Craton. They were formed by the collision of the Congo and the Kaapvaal Cratons between 870 and 550 Ma during the Damara orogeny (Gray et al., 2008; Begg et al., 2009). The Ghanzi-Chobe Belt underwent rifting due to extensional forces during the Kibaran Orogeny collision event, which resulted in the initiation of rifting in Botswana. Cenozoic rifting in the Okavango Rift Zone, which forms the terminus of the southwestern branch of the East African Rift System, was initiated at the boundary between the Ghanzi-Chobe and the Damara Belts (e.g., Leseane et al., 2015).

Botswana also contains two Proterozoic sedimentary basins, the Passarge and Nosop Basins. The Passarge Basin is located in central Botswana, between the Makgadikgadi Line and the Ghanzi-Chobe Belt, and has up to 15 km of sediments deposited during the Neoproterozoic and early Paleozoic era (Key and Ayres, 2000; Pasyanos et al., 2014). The Nosop Basin is located in the southwestern part of Botswana and has sediment thicknesses of up to 15 km as well (Key and Ayres, 2000; Pasyanos et al., 2014) and is comprised of sediments from the Ghanzi and Nama groups. It has been proposed that the Maltahohe Craton, a fragment of the Kalahari Craton extends beneath the Nosop Basin (Wright and Hall, 1990; Begg et al., 2009; Fadel et al., 2018).

### 3. Data and methods

#### 3.1. Gravity data

Bouguer gravity data used in this study were obtained from the Botswana Geoscience Institute (BGI). The gravity data are a compilation of two national-wide gravity surveys from 1972-1973 and 1998-1999 and additional data acquired by different companies. The data have a resolution of ~7.5 km and were provided as a 1 km Bouguer anomaly grid. The Bouguer gravity data (Figure 2A) were then corrected for the effect of sediments, which was removed from the Bouguer anomaly by subtracting the gravitational effect of the sedimentary basins (Figure 2B; Pasyanos et al., 2014). The sediment map has three sedimentary layers with different depth. The reference density model for the sediment correction was set to  $2670 \text{ kg/m}^3$  and density contrasts for the upper (0-1.5 km), middle (between 1.5 km and 5 km) and lower (below 5 km) sediment layers of  $565 \text{ kg/m}^3$ ,  $256 \text{ kg/m}^3$  and  $134 \text{ kg/m}^3$ , respectively, were applied (Pasyanos et al., 2014). The effects of the three layers were calculated according to the density contrast of each layer to the average crustal density (Figure 2C). This resulted in a Bouguer anomaly map corrected for sediments (Figure 2D). The effect of the coarse resolution ( $1^\circ$ ) of the sediment data on the sediment correction is discussed in section 4. The mantle contribution was approximately removed from the sediment corrected Bouguer anomaly by applying a 1000 km Butterworth high-pass filter (Figure 2E; Block et al., 2009). Finally, a 150 km Butterworth low-pass filter was applied to remove high-frequency signals associated with near surface crustal sources. A low pass filter also improves the stability of the gravity inversion, as high frequency data lead to instabilities during the inversion process (Gómez-Ortiz and Agarwal, 2005). Furthermore, it has been shown that gravity data that are subjected to a low pass filter of 150 km contain gravity signals from the Moho (Lefort and Agarwal, 2000). The refined Bouguer gravity data, as shown in Figure 2F, was then used in the regularized inversion process.

#### 3.2. Seismic Constraints

We compiled and used a total number of 53 crustal thickness estimates from previous studies to calibrate the inversion algorithm, and to validate the final crustal thickness model. Twelve stations were obtained from Youssof et al. (2013), twenty-two from Fadel et al. (2018) and nineteen from Yu et al. (2015). These seismic estimates were derived from teleseismic P-wave

receiver function analysis. The locations, crustal thickness ( $H$ ), and  $Vp/Vs$  values of these seismic observations are provided in Table 1.

### 3.3. Gravity inversion

We determined the Moho topography using the regularized inversion algorithm of Uieda & Barbosa (2017). The regularized inversion is based on the Gauss-Newton's formulation of Bott's method (Eq. 1; Bott, 1960; Silva et al., 2014; Uieda & Barbosa, 2017):

$$[A^{kT} A^k + \mu R^T R] \Delta p^k = A^{kT} [g^o(x_i) - g(x_i, \Delta p, p^{k-1})] - \mu R^T R p^k, i = 1, 2, \dots, N; \quad (1)$$

where:

- $\Delta p$  is the density contrast between the crust and the upper mantle,
- $g^o(x_i)$  is the gravity anomaly (input dataset),
- $g(x_i, \Delta p, p^{k-1})$  is the computed gravity anomaly at a point calculated from the Moho depth model, with  $p^{k-1}$  indicating a reference Moho,
- $A^k$  is a Jacobian matrix,
- $\mu$  is a regularization parameter,
- $R$  is a  $L \times M$  finite-difference matrix representing  $L$  first-order differences between adjacent tesseroids, and
- $p^k$  is the  $M$ -dimensional parameter vector containing  $M$ -Moho depths (output dataset).

The regularization parameter ( $\mu$ ) controls the smoothness of the inversion results while maintaining the fit of the solutions with the observed data, via a first-order Tikhonov regularization (Tikhonov and Arsenin, 1977). The Moho topography ( $p^k$ ) contains values that indicate the lateral variation of the crustal structure. The three inversion parameters, a regularization parameter ( $\mu$ ), a reference Moho depth ( $p^l$ ) and density contrast ( $\Delta p$ ), were estimated using a cross-validation approach, called the hold-out method (Kim, 2009). In a first step, the regularization parameter is obtained, which is then used to estimate a reference Moho depth and density contrast. In this approach, gravity data is split into training and testing data. The training data are a dataset based on a regular grid with data at every grid point, twice the

original grid spacing. We set 16 values for the regularization parameter on a logarithmic scale between  $10^{-12}$  and  $10^0$ . Each of the 16 regularization parameters, together with a randomly chosen reference Moho depth of 36 km and a density contrast of  $300 \text{ kg/m}^3$ , were used to invert the training data, and then forward modeled to obtain the calculated gravity anomaly using eq. (1). The randomly chosen input parameters do not affect the final choice of the regularization parameter (Uieda and Barbosa, 2017). The difference between calculated gravity and testing data is evaluated to find the optimal regularization parameter by using the lowest mean square error (MSE)

$$MSE_n = \frac{\|d_{test}^0 - d_{test}^n\|^2}{N_{test}} \dots (2)$$

Where:

- $d_{test}^0$  is the input data (testing data in the case of finding a regularization parameter or seismic crustal thickness data for estimating the reference Moho depth and density contrast),
- $d_{test}^n$  is output dataset (the predicted testing data or crustal thickness values from forward modeling), and
- $N_{test}$  is the number of points in the testing data or the amount of crustal thickness data.

Based on this, a regularization parameter of  $10^{-5}$  was obtained (Figure 3A). This value is similar to other studies where regularization parameters of  $10^{-10}$  to  $10^{-4}$  were found (e.g., Uieda and Barbosa, 2017). Therefore, the obtained value here provides a good estimate for the gravity inversion.

We then used the estimated regularization parameter and seismic observations, as listed in Table 1, to estimate a reference Moho depth and a density contrast that will be used for the gravity inversion. We applied 19 density contrast values between  $200 \text{ kg/m}^3$  and  $650 \text{ kg/m}^3$  with a step of  $25 \text{ kg/m}^3$ . In addition, we defined 36 Moho depth values between 24 km and 60 km with an increment of 1 km. Each of the 684 combinations of reference Moho depths and density contrasts were used as parameters in the inversion of the training data. Topography data from Etopo1 (Amante and Eakins, 2009) was added to the Moho results calculated from each of the

684 combinations. This produced 684 crustal thickness models derived from inversion of the training data. Then, the MSE between gravity derived crustal thickness estimates for each model and the seismic crustal thickness values, as shown in Table 1, was calculated for each of the 684 combinations using Eq. (2). In this comparison, the gravity derived crustal thickness estimates were calculated at the same locations as that of the seismic data points. The lowest MSE, calculated using Eq. 2, was chosen as the reference Moho depth and density contrast, which were subsequently used to invert the refined Bouguer gravity anomaly as optimal parameters (Figure 2F). The comparison produced a reference Moho depth of 36 km and a density contrast of 500 kg/m<sup>3</sup>, as shown in Figure 3B. The input density contrast (500 kg/m<sup>3</sup>) for the inversion assumed the intermediate lower-crustal rocks in Botswana with a density of ~2800 kg/m<sup>3</sup>, relative to the average mantle density of ~3300 kg/m<sup>3</sup> (Warg, 1970).

#### 4. Crustal thickness model

The obtained crustal thickness model of Botswana using a reference Moho depth of 36 km and density contrast of 500 kg/m<sup>3</sup> is presented in Figure 4. The values are within the average crustal thickness estimates for the previous studies in the region, as illustrated in Table 2, and are consistent with seismic observations (Figure 4). In general, the crustal thickness mirrors the refined Bouguer anomaly in most areas, such that low gravity values produce thick crust and vice versa (Van der Meijde et al., 2013). The difference between the observed and calculated gravity fields are concentrated within  $\pm 1$  mGal with a mean value of 0.1 mGal and a standard deviation of 3.02 mGal. This shows a good fit and most of the gravity field can be explained by variations in the crustal thickness. However, uncertainties in the obtained crustal thickness are existent due to the sediment striping approach (Section 3.1). This introduces an uncertainty of ~1.5 km (e.g., Baranov et al., 2017) due to the low resolution ( $1^\circ$ ) of the sediment data (Pasyanos et al., 2014) and interpolation along the edges. The use of a constant density contrast in the gravity inversion can also introduce an uncertainty of up to 3 km in the Moho model (Chisenga et al., 2019; Van der Meijde et al., 2013). Thus, our crustal thickness model overestimates/underestimates the Moho depth by  $\sim \pm 3$  km for every difference of  $\sim \pm 50$  kg/m<sup>3</sup> between the assumed density contrast of 500 kg/m<sup>3</sup> and the actual density contrast between the lower crust and the upper mantle.

The comparison of the gravity derived crustal thickness model to seismic observations (Figure 4A) and other existing crustal thickness models (Table 2) shows a good correlation of results within the accepted error margin. For example, gravity crustal thickness values against seismic observations show that 92.7% of the residuals fall within the accepted margin of  $\pm 6$  km for crustal thickness modeling (e.g., van der Meijde et al., 2013; Van der Meijde et al., 2015). The residuals however, also exhibit a high statistical fit for 56% of the points falling within the range of  $\pm 3$  km (Figures 4A and 4B). Only 5 points of the 53 seismic constraints are outside the  $\pm 6$  km error margin, which are located in the northeastern part of the Okavango Rift Zone and the Zimbabwe Craton. The seismic constraints have, on average, an uncertainty of  $\pm 3$  km with individual seismic studies indicating values of  $\pm 1.5$  km (Fadel et al. 2018),  $\pm 3$  km (Kachingwe et al., 2015), and an average uncertainty of  $\pm 3.1$  km from the work by Yu et al. (2015). The uncertainties of these seismic studies are comparable to the misfit in gravity crustal thicknesses with a standard deviation of  $\pm 3.67$  km.

#### 4.1. Kalahari Craton

In general, the Kalahari Craton is characterized by crustal thicknesses between 39 km and 46 km, and shows the existence of localized zones of slightly-thinned crust of 40 km between relatively thicker crusts of 41-46 km, which are probably related to the intracratonic Bushveld intrusion (Fadel et al., 2018). The crustal thickness beneath the Zimbabwe Craton is 38-45 km and a thinner crust is visible in the northwest towards the Northern Marginal Zone of the Limpopo-Shashe Belt. On average the crust is roughly 40-42 km thick in the Zimbabwe Craton. Seismic studies obtained values between 40 and 50 km (e.g., Fadel et al., 2018; Yousof et al., 2013), which is slightly larger than the results obtained from gravity data. The velocity ratio obtained from seismic data ( $V_p/V_s$  of 1.69 - 1.75; Table 1) point to a felsic lower crust, which translates to a higher density contrast to the upper mantle, relative to the assumed lower crustal density of  $2800 \text{ kg/m}^3$  (Section 3.3). The area also has a highly complex lower crust, which makes it difficult to identify the Moho (e.g., Nguuri et al., 2001). The thinner crust could be caused by reworking of crustal materials during the Okavango dyke emplacement. A crustal thickness of 38-45 km is obtained beneath the Kaapvaal Craton, with an average crustal thickness of 41 km. The crustal thickness from gravity data is comparable to previous studies (Table 2). The craton has a relatively thin crust along the boundary within orogenic belts.

#### 4.2. Congo Craton and its transition to Damara Belt

The Congo Craton shows a crustal thickness of 39-46 km, with an average of 41 km. The average thickness slightly differs with 39 km and 38 km for Archean cratonic crust based on results from Kachingwe et al. (2015) and Fadel et al. (2018), respectively. However, our estimates are consistent with results from Yu et al. (2015) on the south-eastern side of the Congo Craton. We also identified a 40 km stretched kidney shaped belt within the Damara Belt that wraps the edges of the proposed Congo Craton. The relatively thin crust on the edges of the Congo Craton suggests a reworked Damara Belt as a result of the collision of the Congo and the Kalahari Cratons during the Pan-African and the Damara orogeny (Gray et al., 2008). Based on gravity observations, we suggest that the thicker crust (~ 46 km) to the northwest represents an over-thrust collisional zone in which the Damara Belt lies on top of the Congo Craton. This hypothesis is supported by presence of the relatively thicker crust in the proposed Congo Craton with similar average crustal thickness values for both stable Archean and Proterozoic mobile belts in Africa as discussed by Tugume et al. (2013). The area is overlain by Proterozoic rocks within the proposed Archean Congo Craton in Botswana (Key & Ayres, 2000; Singletary et al., 2003). Finally, the lithospheric extent of the proposed cratonic region is located beneath the Proterozoic region of the Damara Belt, as resolved from the magnetotelluric study by Khoza et al. (2013). Khoza et al. (2013) suggested that the Congo Craton extended further south into south-western Botswana without giving the finite boundary. We however, place the boundary between the relatively thicker Congo Craton and the thinner Damara crust on the north-western edge of the kidney-shaped 40 km thick crust (Figure 4A). This interpretation is also consistent with the boundary of the Congo Craton derived from seismic tomography studies (Yu et al., 2017; Lebedev et al., 2020).

#### 4.3. Limpopo-Shashe Belt

The Limpopo-Shashe Belt has crustal thicknesses between 40 and 46 km. This is comparable to two estimates from Yu et al. (2015), which identified a 43.5 km and 44.5 km thick crust. The Limpopo-Shashe Belt has the thickest crust (46 km) within the Central Zone and relatively thinner crustal thicknesses (40 km) in the Northern Marginal Zone and the Southern Marginal

Zone. The thicker crust in the Central Zone represents a pop-up structure related to the collision of the Zimbabwe Craton and the Kaapvaal Craton, similar to the Himalayan style collision (Roering et al., 1992; Ranganai et al., 2002; Fadel et al., 2018). The thick crust agrees with previous studies on post-Archean reworked belts in the Kalahari Craton, which resulted in a ~45-50 km thick crust (e.g., Nguuri et al., 2001). However, seismic studies (e.g., Nguuri et al., 2001; Fadel et al., 2018; Youssof et al., 2013) indicated that the collisional zone was located slightly to the north of our results. This difference could be due to the seismic-stations coverage of the previous studies in the peripheral of the 46 km thick crust resolved by gravity data, as shown in Figure 4A.

The April 3<sup>rd</sup>, 2017, Botswana earthquake is located in the Southern Marginal Zone, which is characterized by a relatively thin crust in this region. However, the crust slightly thickens towards the southeast, from 40 km to 41 km along the boundary with the Kaapvaal Craton. Unlike the Central Zone and the Northern Marginal Zone, the Southern Marginal Zone has undergone only a single metamorphic event at 2.72–2.65 Ga (e.g., Roering et al., 1992). The current crustal structure in this region could possibly be inherited from past processes, as no evidence from rock dating shows other tectonic or metamorphic events in recent times (Droop, 1989; Roering et al., 1992). The Northern Marginal Zone shows little variation in the crustal thickness. This flat crust could indicate little deformation and extension, which is similar to the surrounding Zimbabwe Craton.

#### **4.4. Ghanzi-Chobe Zone**

We observe a crustal thickness of 35-46 km for the Ghanzi-Chobe Zone. The thickest crust (46 km) in the southwestern Ghanzi-Chobe Zone could be related to the collision of the Congo and the Kalahari Cratons (Gray et al., 2008). The northeastern end of the Ghanzi-Chobe is thinner, which is perhaps related to an extension associated with the East African Rift System. The Okavango Rift Zone starts from the Damara Belt into the Ghanzi-Chobe Zone (Yu et al., 2015b), with an average crustal thickness of ~38 km in relation to the surrounding 40 - 43 km thick crust, representing a thinning of 2 – 5 km (Figure 4A). The Okavango Rift Zone has a mafic lower crust with  $V_p/V_s$  of > 1.81, which reaches a maximum of 1.95 (Christensen, 1996; Fadel et al., 2018). Such a high-density lower crust, relatively to the assumed intermediate density lower

crust in our inversion, results in crustal thickness variations and high deviation in the Okavango Rift Zone. Rifting patterns in the Okavango Rift Zone are barely visible apart from the north-eastern side of the region. However, a relatively localized thin crust, which is close to point B15, surrounded by thick crust between the northeastern Damara Belt and the northeastern Passarge Basin is visible in the central Okavango Rift Zone. This indicates a possible underdeveloped or immature rift zone of the Okavango Rift Zone. Our crustal thickness estimates (36 km) differ considerable from gravity crustal thickness obtained from a 2D-spectral radial analysis (~30 km; Leseane et al., 2015) but are in agreement with seismic data in this region, as shown in Figure 4A. Fadel et al. (2018) also noted this significant difference between the crustal thickness values of Leseane et al. (2015) and Yu et al. (2015).

#### **4.5. Magondi-Okwa-Xade-Kheis Belts**

The Magondi-Okwa-Xade-Kheis Belts were influenced by the Kalahari Suture Zone during their formation. They form a Paleoproterozoic boundary with the Kalahari Craton and the Damara-Ghanzi-Chobe Belts (Figure 1). Unsurprisingly, the Kheis-Okwa-Xade-Magondi Belt shows a crustal thickness of 37-44 km with an average of ~41 km. The thinnest crust is located in the Xade and the Kheis Belts, while the Okwa Block and the northwestern part of the Magondi Belt show a ~42 km relatively thicker crust. The crustal thickness values in the Kheis Belt reach a maximum of 43 km in the south. The Magondi Belt has an almost stretched/flat crust in the middle, which increases in thickness toward the north and the Limpopo-Shashe Belt. The thick crust of the Okwa Block bulges out in relation to the other Paleoproterozoic crusts, possibly representing a post-Archaean reworking on the boundary of the cratonic regions during the Eburnean Orogeny similar to the Limpopo-Shashe Belt.

#### **4.6. Sedimentary Basins**

The thinnest crust underlies the Proterozoic Nosop and Passarge Basins. The basins show a considerable thin crust below the thick sediment layers. The observed crustal thickness for the Nosop Basin is 35-42 km with an average of 38 km. The Nosop Basin crustal thickness does not match the gravity observations, but strongly mirrors the sediment thickness map, which indicates the effect of sediments correction in this region. The absence of seismic observations in the

Nosop Basin means that we do not have independent constraints to check the thickness validity. The observed crustal thickness for the Passarge Basin is 36-43 km. The thin crust beneath the Passarge Basin extends southeastwards to the Limpopo-Shashe Belt through the Magondi Belt. It then bifurcates around the 46 km thick Central Zone into the Northern Marginal Zone and the Southern Marginal Zone. The northern arm of the bifurcated thin crust coincides with the location of the Okavango dyke swarm at the boundary of the Zimbabwe Craton and the Northern Marginal Zone (Figure 4A). In the Southern Marginal Zone, the southern arm of the bifurcated thin crust underlies the Moiyabana Epicentral Region of the  $M_w$  6.5 2017 Botswana earthquake (Figure 4 and 5).

## 5. Implication to the 3<sup>rd</sup> April 2017, Botswana Earthquake

Our results reveal a crustal thickness of ~ 40 km for the epicenter of the April 3<sup>rd</sup>, 2017  $M_w$  6.5 Botswana earthquake (Figure 5), flanked by a 43 km thick Kaapvaal Craton to the southwest and a 46 km pop-up structure in the Central Zone of the Limpopo-Shashe Belt to the northeast (Figure 5). The aftershocks, with hypocenter of deeper than 15 km, also cluster along this relatively thin crustal zone. The crustal thickness lateral variation in this region (Figure 5) is consistent with the revealed structural geometry of the Moiyabana Epicentral Region (Figure 5; Kolawole et al., 2017). The causative fault inferred from InSAR data (Kolawole et al., 2017) lies at the thinnest crust in this region of 40 km. The structural geometry of the Paleoproterozoic thrust faults (Kolawole et al., 2017) coincides with the northwestern widening of the relatively thin crust, indicating a tectonic relationship between crustal thickness and fault geometry. Thus, Fault orientation and formation in this region could be partially controlled by the local crustal thickness variation. Further, it is observed that the southeastern end of the causative fault and the epicenter of the  $M_w$  6.5 Botswana earthquake are located on the southern arm of the bifurcated thin crust (Figure 4A). The width of the relatively thin crust in this part is small, and then it widens in the northwestern direction towards the Magondi Belt. The southeastern part of the Southern Marginal Zone of the Magondi Belt is relatively thicker with almost uniform crustal thickness (Figures 4A and 5). This could suggest that the relatively thinner crust in the epicentral region has undergone possible recent tectonic activities, which might have contributed to the occurrence of the Botswana Earthquake. The relatively thinner region also shows consistency with the local stress regime as indicated by the focal mechanisms (Bird et al., 2006; Kolawole et

al., 2017), which suggests that the thinning crust could be due to extensional forces as the results of the recent tectonic activities.

The relatively thin crust in the Moiyabana Epicentral region extends and connects to the relatively thin crust in the Passarge Basin and the northeastern end of the Okavango Rift Zone (Figure 6A). These regions show shallow Curie Point Depth (CPD), which indicates elevated levels of heat flows (Kolawole et al., 2017; Leseane et al., 2015). The comparison to the crustal thickness and heat flow information indicates that a shallow CPD of ~10 km correlates spatially with the 40 km relatively thin crust in comparison to a 43 km thick crust in the northeastern part that is associated with a relatively deeper CPD of ~30 km. The pattern of the local crustal thickness variations is also consistent with global CPD values that show shallow CPD (<20 km) in relation to thin crusts (~40 km; Figure 6B). In addition, a relatively thin crust at the northeastern tip of Botswana in the Okavango Rift Zone is correlated with a low shear-wave velocity zone in the mantle (~150 km), which is interpreted as the East African Rift System (EARS) expression at northern Botswana (Fadel, 2018; Fadel et al., 2020). Fadel et al. (2020) have suggested that the EARS expression at the northern tip of Botswana extends to the Incipient Okavango Rift region and the Moiyabana Epicentral regions through weak crustal zones. These weak crustal zones facilitate the moving of the ascending hot fluids/fluids from the EARS causing elevated heat flow and shallow CPDs, which are postulated to trigger earthquakes in the Okavango Rift Zone (Leseane et al., 2015). Moreover, this could explain the Botswana earthquake in the Moiyabana Epicentral Region, as explained below.

We therefore propose the following mechanism for the Botswana earthquake. At the Moiyabana Epicentral Region, the weak crust and mantle (Moorkamp et al., 2019) and the local stress regime (Bird et al., 2006; Stamps et al., 2010; Stamps et al., 2014) lead to a relative thinning of the crust, compared to the surrounding, as observed in the Moiyabana Epicentral Region. The thermal fluids from the East African Rift System (Fadel et al., 2020) probably erodes the lower crust during the migration process, which results in a thin crust as observed from the crustal thickness model (e.g., Mckenzie et al., 2000; Reyners et al., 2007). As explained, the thin crust controlled the fault geometry that resulted in the enhancement of the movement of the thermal fluids that caused the observed elevated heat flow and shallow CPD revealed from previous

studies (Ballard et al., 1987; Kolawole et al., 2017). The pre-existing conditions, coupled with the existing local stress regime, accumulate beneath the Moiyabana Epicentral Region that could have led to a possible tectonic reactivation of the weak zone within the thin crust of the Southern marginal Zone. Thus, we suggest that the Southern Marginal Zone of the Limpopo-Shashe Belt is a possible tectonic extension zone in which different parameters play a role and could be a source for future occurrences of earthquakes.

## 6. Conclusion

The ground and airborne gravity data have facilitated the construction of a crustal thickness model of Botswana, which has enabled us to study the crustal architecture beneath the thick Kalahari cover. The results revealed a relatively thin crust (35-40 km) in the Okavango Rift Zone and sedimentary basins, and a thicker crust (41-46 km) in cratonic regions and orogenic belts. The average thicknesses of the tectonic terranes in Botswana are within the average range of crustal thicknesses in Africa, and are comparable to the seismically derived crustal thickness model of Botswana produced by Fadel et al. (2018). The crustal structure revealed localized regions of relatively thin crust in cratonic regions between two regions with thicker crusts. One such thinned region is the Moiyabana Epicentral Region of the April 3<sup>rd</sup>, 2017, Botswana earthquake. The crustal thickness lateral variations are consistent with the fault geometry, shallow CPD and elevated heat flow in the Moiyabana Epicentral Region. The thin crust in the Moiyabana Epicentral Region was suggested to have occurred due to erosion of the lower crust as the result of thermal fluids movement from the mantle of the East African Rift System and a persistent local stress regime acting on the region. We proposed that the combined effect of the presence of a thin crust, thermal fluids, elevated heat flow, and its similarity to a predicted local stress regime in the Moiyabana Epicentral Region along the cratonic edges and a deep seismic source contributed to the occurrence of the Botswana earthquake. It is suggested that the region is a possible tectonic extension zone that could lead to future occurrences of earthquakes.

## Acknowledgment

We thank the Botswana Geoscience Institute (BGI), formerly the Geological Survey of Botswana, for providing the gravity data. We also thank the editor, Ling Chen, and two anonymous reviewers that helped to improve the manuscript. This research was supported by a

grant provided by Netherlands Organization for Scientific Research (NWO), grant number ALW-GO-AO/11-30, National Scientific Foundation of China (Grant No. U1831132 and 41374024) and Innovation Group of Natural Fund of Hubei province (Grant No. 2018CFA087)

## Reference

- Albano, M., Polcari, M., Bignami, C., Moro, M., Saroli, M., Stramondo, S., 2017. Did Anthropogenic Activities Trigger the 3 April 2017 Mw 6.5 Botswana Earthquake? *Remote Sens.* 9, 1028. doi:10.3390/rs9101028
- Albaric, J., D'everch`ere, J., Petit, C., Perrot, J., Gall, B. Le, 2003. Crustal rheology and depth distribution of earthquakes: Insights from the central and southern East African Rift System. *Tectonics* 468, 28–41.
- Amante, C., Eakins, B.W., 2009.ETOPO1 1 Arc-Minute Global Relief Model: Procedures, Data Sources and Analysis, NOAA Technical Memorandum NESDIS NGDC-24,. Boulder, Colorado, USA.
- Ballard, S., Pollack, H.N., Skinner, N.J., 1987. Terrestrial Heat-Flow in Botswana and Namibia. *J. Geophys. Res. Earth Planets* 92, 6291–6300. doi:10.1029/JB092iB07p06291
- Baranov, A., Tenzer, R., Bagherbandi, M., 2017. Combined Gravimetric – Seismic Crustal Model, *Surveys in Geophysics*. Springer Netherlands. doi:10.1007/s10712-017-9423-5
- Begg, G.C., Griffin, W.L., Natapov, L.M., O'Reilly, S.Y., Grand, S.P., O'Neill, C.J., Hronsky, J.M.A., Djomani, Y.P., Swain, C.J., Deen, T., Bowden, P., 2009. The lithospheric architecture of Africa: Seismic tomography, mantle petrology, and tectonic evolution. *Geosphere* 5, 23–50. doi:10.1130/GES00179.1
- Bird, P., Ben-Avraham, Z., Schubert, G., Andreoli, M., Viola, G., 2006. Patterns of stress and strain rate in southern Africa. *J. Geophys. Res. Solid Earth* 111, 1–14. doi:10.1029/2005JB003882
- Block, A.E., Bell, R.E., Studinger, M., 2009. Antarctic crustal thickness from satellite gravity: Implications for the Transantarctic and Gamburtsev Subglacial Mountains. *Earth Planet.*

Sci. Lett. 288, 194–203. doi:10.1016/j.epsl.2009.09.022

Bott, M.H.P., 1960. The use of rapid digital computing methods for direct gravity interpretation of sedimentary basins. Geophys. J. Int. 3, 63–67.

Calais, E., Camelbeeck, T., Stein, S., Liu, M., Craig, T.J., 2016. A new paradigm for large earthquakes in stable continental plate interiors. Geophys. Res. Lett. 20, 10,621–10,637. doi:10.1002/2016GL070815

Chisenga, C., Yan, J., Yan, P., 2019. A crustal thickness model of Antarctica calculated in spherical approximation from satellite gravimetric data. Geophys. J. Int. 218, 388–400. doi:10.1093/gji/ggz154

Christensen, I., 1996. Poisson's ratio and crustal seismology. J. Geophys. Res. Solid Earth 101, 3139–3156.

Clifford, T.N., 1970. The structural framework of Africa, in: Clifford, T.N., Gass, I.G. (Eds.), African Magmatism and Tectonics. Oliver and Boyd, Edinburgh, pp. 1–26.

Craig, T.J., Jackson, J.A., Priestley, K., Venzie, D.M., 2011. Earthquake distribution patterns in Africa: their relationship to variations in lithospheric and geological structure, and their rheological implications. Geophys. J. Int. 185, 403–434. doi:10.1111/j.1365-246X.2011.04950.x

Droop, G.T.R., 1989. Reaction history of garnet-sap- phirine granulites and conditions of Archaean high-pressure granulite-facies metamorphism in the central Limpopo mobile belt, Zimbabwe. J. Metamorph. Geol. 7, 383–403. doi:10.1111/j.1525-1314.1989.tb00604.x

Fadel, I., 2018. Crustal and upper mantle structure of Botswana : is Botswana rifting ? PhD Thesis, ITC-University of twente.

Fadel, I., Meijde, M. Van Der, Paulssen, H., 2018. Crustal Structure and Dynamics of Botswana. J. Geophys. Res. Solid Earth 123, 10,659–10,671. doi:10.1029/2018JB016190

Fadel, I., Paulssen, H., Meijde, M. Van Der, Motsamai, T., Ntibinyane, O., Nyblade, A.A., 2020.

Crustal and upper mantle shear wave velocity structure of Botswana: the April 3, 2017 central Botswana earthquake linked to the East African Rift System. *Geophys. Res. Lett.* In press.

Gao, S.S., Liu, K.H., Reed, C.A., Yu, Y., Massinque, B., Mdala, H., Moidaki, M., Mutamina, D., Atekwana, E.A., Ingate, S., Reusch, A.M., 2013. Seismic arrays to study African rift initiation. *Eos, Trans. Am. Geophys. Union* 94, 213–214.

Gardonio, B., Jolivet, R., Calais, E., Lecl, H., 2018. The April 2017 M w 6 . 5 Botswana Earthquake : An Intraplate Event Triggered by Deep Fluids. *Geophys. Res. Lett.* doi:10.1029/2018GL078297

Gómez-Ortiz, D., Agarwal, B.N.P., 2005. 3DINVER.M: a MATLAB program to invert the gravity anomaly over a 3D horizontal density interface by Parker–Oldenburg’s algorithm. *Comput. Geosci.* 31, 513–520. doi:10.1016/j.cageo.2004.11.004

Gray, D.R., Foster, D., Meert, J., Goscombe, E., Armstrong, B., Trouw, R., Passchier, C., 2008. A Damara orogen perspective on the assembly of south- western Gondwana. *Geol. Soc. London, Spec. Publ.* 294, 257–278

Kachingwe, M., Nyblade, A., Julià, J., 2015. Crustal structure of Precambrian terranes in the southern African subcontinent with implications for secular variation in crustal genesis. *Geophys. J. Int.* 202, 535–547. doi:10.1093/gji/ggv136

Key, R.M., Ayres, N., 2009. The 1998 edition of the National Geological Map of Botswana. *J. African Earth Sci.* 30, 427–451. doi:10.1016/S0899-5362(00)00030-0

Khoza, T.D., Jones, A.G., Muller, M.R., Evans, R.L., Miensopust, M.P., Webb, S.J., 2013. Lithospheric structure of an Archean craton and adjacent mobile belt revealed from 2-D and 3-D inversion of magnetotelluric data: Example from southern Congo craton in northern Namibia. *J. Geophys. Res.* 118, 4378–4397. doi:10.1002/jgrb.50258

Kim, J.H., 2009. Estimating classification error rate: repeated cross-validation, repeated hold-out and bootstrap. *Comput. Stat. data Anal.* 53, 3735–3745.

- Kolawole, F., Atekwana, E.A., Malloy, S., Stamps, D.S., Grandin, R., Abdelsalam, M.G., Leseane, K., Shemang, E.M., 2017. Aeromagnetic, gravity, and Differential Interferometric Synthetic Aperture Radar analyses reveal the causative fault of the 3 April 2017 Mw 6.5 Moiyabana, Botswana, earthquake. *Geophys. Res. Lett.* 44, 8837–8846. doi:10.1002/2017GL074620
- Lebedev, S., Schaeffer, A.J., Gaina, C., 2020. African cratonic lithosphere carved by mantle plumes. *Nat. Commun.* 11, 92. doi:10.1038/s41467-019-13871-2
- Lefort, J.P., Agarwal, B.N.P., 2000. Gravity and geomorphological evidence for a large crustal bulge cutting across Brittany (France): A tectonic response to the closure of the Bay of Biscay. *Tectonophysics* 323, 149–162. doi:10.1016/S0040-1951(00)00103-7
- Leseane, K., Atekwana, Estella A, Mickus, K.L., Abdelsalam, M.G., Shemang, E.M., Atekwana, Eliot A, 2015. Thermal perturbations beneath an incipient Okavango Rift Zone, northern Botswana. *J. Geophys. Res. Solid Earth* 120, 1210–1228. doi:10.1002/2014JB011029
- Li, C., Lu, Y., Wang, J., 2017. A global reference model of Curie- point depths based on EMAG2. *Sci. Rep.* 1–9. doi:10.1038/srep45129
- Materna, K., Wei, S., Wang, X., Feng, L., Wang, T., Chen, W., Salman, R., Bürgmann, R., 2019. Source characteristics of the 2017 M w 6 . 4 Moijabana , Botswana earthquake , a rare lower-crustal event within an ancient zone of weakness. *Earth Planet. Sci. Lett.* 506, 348–359. doi:10.1016/j.epsl.2018.11.007
- McCourt, S., Van Reenen, D., Roering, C., Smit, A., 1995. Geological constraints on the Limpopo Orogeny, Geological Society of South Africa, Abstracts Centennial Geocongress. Johannesburg.
- Mckenzie, D., Nimmo, F., Jackson, J.A., 2000. Characteristics and consequences of flow in the lower crust. *J. Geophys. Res.* 105, 11,029-11,046.
- Midzi, V., Saunders, I., Manzunzu, B., Kwadiba, M.T., Zulu, S., Jele, V., Mantsha, R., Marimira, K.T., Mulabisana, T.F., Ntibinyane, O., Pule, T., Rathod, G.W., Sitali, M., Tabane, L., Van, G., 2018. The 03 April 2017 Botswana M6.5 earthquake: Preliminary results. *J. African*

Earth Sci. 143, 187–194. doi:10.1016/j.jafrearsci.2018.03.027

Mooney, W.D., Ritsema, J., Keun, Y., 2012. Crustal seismicity and the earthquake catalog maximum moment magnitude (M<sub>cmax</sub>) in stable continental regions (SCRs): Correlation with the seismic velocity of the lithosphere. *Earth Planet. Sci. Lett.* 357–358, 78–83. doi:10.1016/j.epsl.2012.08.032

Moorkamp, M., Fishwick, S., Walker, R.J., Jones, A.G., Mt, C., 2019. Geophysical evidence for crustal and mantle weak zones controlling intra-plate seismicity – the 2017 Botswana earthquake sequence. *Earth Planet. Sci. Lett.* 506, 175–183. doi:10.1016/j.epsl.2018.10.048

Nguuri, T.K., Gore, J., James, D.E., Webb, S.J., Wright, C., 2001. crustal structure beneath southern Africa and its implications for the formation and evolution of the Kaapvaal and Zimbabwe cratons. *Geophys. Res. Lett.* 28, 2501–2504.  
doi:10.1029/2000GL012587.GEOPHYSICAL

Nguuri, T. K., Gore, J., James, D.E., Webb, S.J., Wright, C., Zengeni, T.G., Gwava, O., Snoke, J. a., 2001. Crustal structure beneath southern Africa and its implications for the formation and evolution of the Kaapvaal and Zimbabwe cratons. *Geophys. Res. Lett.* 28, 2501–2504. doi:10.1029/2000GL012587

Nyblade, A., Dirks, P., 2006. AfricaArray Seismic Network. *AfricaArray Newslett.*  
[https://doi.org/http://africaarray.psu.edu/publications/newsletters/2006\\_Web.pdf](https://doi.org/http://africaarray.psu.edu/publications/newsletters/2006_Web.pdf)

Nyblade, A.A., Langston, C.A., 1995. East African earthquakes below 20 km depth and their implications for crustal structure. *Geophys. J. Int.* 121, 49–62.

Pasyanos, M.E., Masters, T.G., Laske, G., Ma, Z., 2014. LITHO1.0: An updated crust and lithospheric model of the Earth. *J. Geophys. Res. Solid Earth* 119, 2153–2173.  
doi:10.1002/2013JB010626.Received

Ranganai, R.T., Kampunzu, A.B., Atekwana, E.A., Paya, B.K., King, J.G., Koosimile, D.I., Stettler, E.H., 2002. Gravity evidence for a larger Limpopo Belt in southern Africa and geodynamic implications. *Geophys. J. Int.* 149. doi:10.1046/j.1365-246X.2002.01703.x

- Reeves, C. V., Hutchins, D.G., 1982. A progress report on the geophysical exploration of the Kalahari in Botswana. *Geoexploration* 20, 209–224. doi:10.1016/0016-7142(82)90022-9
- Reyners, M., Eberhart-phillips, D., Stuart, G., 2007. The role of fluids in lower-crustal earthquakes near continental rifts. *Nature* 446, 1075–1078. doi:10.1038/nature05743
- Roering, C., Reenen, D.D. Van, Smit, C.A., Jr, J.M.B., Beer, J.H. De, Wit, M.J. De, 1992. Tectonic model for the evolution of the Limpopo Belt. *Precambrian Res.* 55, 539–552. doi:10.1016/0301-9268(92)90044-O
- Saria, E., Calais, E., Stamps, D.S., Delvaux, D., Hartnady, C.J.H., 2014. Present-day kinematics of the East African Rift. *J. Geophys. Res. Solid Earth* 119, 3584–3600. doi:10.1002/2013JB010901.Abstract
- Schaller, M., 1999. Exhumation of Limpopo Central Zone granulites and dextral continent-scale transcurrent movement at 2.0 Ga along the Pavia Shear Zone, Northern Province, South Africa. *Precambrian Res.* 96, 263–288. doi:10.1016/S0301-9268(99)00015-7
- Shudofsky, G.N., Cloetingh, S., Stein, S., Wortel, R., 1987. Unusually deep earthquakes in East Africa: Constraints on the thermo-mechanical structure of a continental rift system. *Geophys. Res. Lett.* 14, 741–744.
- Silva, J., Santos, D., Gomes, K., 2014. Fast gravity inversion of basement relief. *Geophysics* 79, G79–G91.
- Simon, R., Kwadiba, M., King, J., Moidaki, M., 2012. A history of Botswana's seismic network. *Botsw. Notes Rec.* 44, 184–192.
- Singletary, S.J., Hanson, R.E., Martin, M.W., Crowley, J.L., Bowring, S.A., Key, R.M., Ramokate, L. V., Direng, B.B., Krol, M.A., 2003. Geochronology of basement rocks in the Kalahari Desert, Botswana, and implications for regional Proterozoic tectonics. *Precambrian Res.* 121, 47–71. doi:10.1016/S0301-9268(02)00201-2
- Sloan, R.A., Jackson, J.A., Kenzie, D.M., Priestley, K., 2011. Earthquake depth distributions in central Asia, and their relations with lithosphere thickness, shortening and extension.

Geophys. J. Int. 185, 1–29. doi:10.1111/j.1365-246X.2010.04882.x

Stamps, D.S., Flesch, L.M., Calais, E., 2010. Lithospheric buoyancy forces in Africa from a thin sheet approach. *Int. J. Earth Sci.* 99, 1525–1533. doi:10.1007/s00531-010-0533-2

Stamps, D.S., Flesch, L.M., Calais, E., Ghosh, A., 2014. Solid Earth Current kinematics and dynamics of Africa and the East. *J. Geophys. Res.* 1–26.  
doi:10.1002/2013JB010717.Received

Talwani, P., 2014. Intraplate Earthquakes. Cambridge university press, New York.

Tesauro, M., Kaban, M.K., Mooney, D.W., 2015. Variations of the lithospheric strength and elastic thickness in North America. *Geochemistry, Geophysics, Geosystems* 16, 2197–2220.  
doi:10.1002/2015GC005937.Received

Tikhonov, A.N., Arsenin, V.Y., 1977. Solutions of Ill-Posed Problems. Winston and Sons, Washington DC.

Tugume, F., Nyblade, A., Julià, J., van der Meijde, M., 2013. Precambrian crustal structure in Africa and Arabia: Evidence lacking for secular variation. *Tectonophysics* 609, 250–266.  
doi:10.1016/j.tecto.2013.04.027

Uieda, L., Barbosa, V.C.F., 2017. Fast nonlinear gravity inversion in spherical coordinates with application to the South American Moho. *Geophys. J. Int.* 208, 162–176.  
doi:10.1093/gji/ggw350

van der Meijde, M., Fadel, I., Ditmar, P., Hamayun, M., 2015. Uncertainties in crustal thickness models for data sparse environments: A review for South America and Africa. *J. Geodyn.* 84. doi:10.1016/j.jog.2014.09.013

Van der Meijde, M., Julià, J., Assumpção, M., 2013. Gravity derived Moho for South America. *Tectonophysics* 609, 456–467. doi:10.1016/j.tecto.2013.03.023

Wang, C., 1970. Density and Constitution of the Mantle. *J. Geophys. Res.* 75.

Wijk, J.W. Van, 2005. Role of weak zone orientation in continental lithosphere extension.

Geophys. Res. Lett. res 32, 1–4. doi:10.1029/2004GL022192

Wright, J.A., Hall, J., 1990. Deep Seismic profiling in the Nosop Basin, Botswana: cratons, mobile belts and sedimentary basins. *Tectonophysics* 173, 333–343. doi:10.1016/0040-1951(90)90228-Z

Youssouf, M., Thybo, H., Artemieva, I.M., Levander, A., 2013. Moho depth and crustal composition in Southern Africa. *Tectonophysics* 609, 267–287. doi:10.1016/j.tecto.2013.09.001

Yu, Y., Gao, S.S., Moidaki, M., Reed, C.A., Liu, K.H., 2015a. Seismic anisotropy beneath the incipient Okavango rift: Implications for rifting initiation. *Earth Planet. Sci. Lett.* 430, 1–8.

Yu, Y., Liu, K., Moidaki, M., Mickus, K., Atekwana, F.A., Gao, S.S., 2015b. A joint receiver function and gravity study of crustal structure beneath the incipient Okavango Rift, Botswana. *Geophys. Res. Lett.* 42, 8398–8405.

Yu, Y., Liu, K.H., Huang, Z., Zhao, D., Reed, C.A., Moidaki, M., Lei, J., Gao, S.S., 2017. Mantle structure beneath the incipient Okavango rift zone in southern Africa. *Geosphere* 13, 102–111. doi:10.1130/GES01331.1

## Figure Caption

Figure 1: Precambrian tectonic map of Botswana, modified after Key & Ayres, (2000), Ranganai et al., (2002) and Singletary et al., (2003). The white polygon indicates the extent of the Okavango Rift Zone after Yu et al. (2015). Also shown are the distribution of seismic stations as yellow, green and red triangles (Youssouf et al., 2013; Yu et al., 2015; Fadel et al., 2018). The blue star shows the location of the Mw 6.5 Botswana earthquake of April 3<sup>rd</sup>, 2017.

Figure 2: (A) Bouguer anomaly map; (B) Sediment thickness map (Pasyanos et al., 2014); (C) Map of gravitational effect calculated from the three sedimentary layers; (D) Bouguer anomaly corrected for sediments; (E) Sediment corrected Bouguer gravity data with a high pass (1000 km) filter applied to it; (F) Refined Bouguer anomaly map obtained after the application of low-

pass (150 km) and high-pass (1000 km) filters to the sediment corrected Bouguer anomaly from (E).

Figure 3: Regularized gravity inversion results. Optimum value is indicated by a red box. (A) Regularized curve from the cross-validation for the estimation of the regularization parameter ( $10^{-5}$ ). (B) Cross-validation results to obtain the reference Moho depth (36 km) and density contrast ( $500 \text{ kg/m}^3$ ).

Figure 4: (A) The gravity derived crustal thickness estimates overlain by the tectonic map of Botswana. The points indicate the difference between the gravity based crustal thickness and seismic observations shown in Table 1. Also shown are the extent of the Okavango Rift Zone and normal faults within the white polygon as well as the Moiyabana Epicentral Region of the Botswana earthquake (black rectangle), and the delineated faults from InSAR, gravity and magnetic data after Kolawole et al. (2017). The epicentral region is highlighted by black outlined triangle that is presented in Figure 5 below; the boundary of Congo Craton is placed on the northwestern end of the kidney-shaped feature within the Damara belt based on the results of this study. (B) The scatterplot of the misfits between the seismic observations on the y-axis and the gravity derived estimates on the x-axis. The blue line indicates 0 km, the green line indicates 3 km, and the red line indicates 6 km deviations.

Figure 5: Crustal thickness of the Moiyabana Epicentral Region. Also shown are fault geometry after Kolawole et al. (2017) and the location of April 3<sup>rd</sup>, 2017,  $M_w$  6.5 earthquake (mainshock) and several aftershocks with magnitude  $M_w$  of  $< 5$ . The white solid line represents tectonic terrane boundaries and the white dashed line represents subterranean boundaries within the Limpopo-Shashe Belt.

Figure 6: (A) Crustal thickness map that covers the Okavango Rift Zone and Moiyabana Epicentral Region. (B) Curie Point Depth (CPD) map of the same area after Li et al. (2017). Also shown are the heat flow values from borehole data, represented by yellow circles, after Ballard et al. (1987) and the connection of the Okavango Rift Zone and Moiyabana Epicentral Region as blue dashed lines after Fadel et al. (2020). The black dashed line represents faults in the Okavango Rift Zone, and the white line shows terrane boundaries.

**Table Caption**

Table 1: Summary of the values derived from local and teleseismic receiver functions. H in the table represents crustal thickness values in kilometers (km). Seismic observations are summarized in tectonic terranes according to their spatial location as they appear in the tectonic map of Botswana, as shown in Figure 1.

Table 2: Summary of the comparison of our gravity model with other existing models in km

<b>Tectonic Regime</b>	<b>Fadel et al. (2018)</b>			<b>Yu et al. (2015)</b>			<b>Youssouf et al. (2013)</b>		
	Station	H	V <sub>p</sub> /V <sub>s</sub>	Station	H	V <sub>p</sub> /V <sub>s</sub>	Station	H	V <sub>p</sub> /V <sub>s</sub>
Zimbabwe Craton	NE217	40	1.78				SA71	40.5	1.80
	NE218	49	1.69				SA70	50.5	1.75
Kaapvaal Craton	LBTB	42	1.75				SA59	41.5	1.78
	NE201	36	1.81				SA60	41.5	1.77
	NE212	39	1.74				SA61	43.5	1.67
	NE213	39	1.67				SA62	40.5	1.8
	NE221	39	1.67				SA63	43	1.79
	NE204	38	1.79	B12	46.2	1.77			
Congo Craton	NE207	38	1.71	B13	46.6	1.75			
				B14	45.8	1.80			
Limpopo-Shashe Belt	NE219	42	1.72	B02	42.8	1.73	SA64	41	1.75
	NE208	40	1.69	SA66	44.7	1.81	SA65	43	1.75
				B01	43.7	1.81	SA66	46.5	1.77
				B16	42.6	1.75	SA67	39.5	1.79
				SA64	41.5	1.73	SA68	41	1.87
				SA65	42.7	1.75			
Magondi Belt	NE216	37	1.75	B04	42.6	1.76			
				B03	40.8	1.76			
Kheis Belt	NE202	39	1.71						
Okwa Block	NE211	44	1.72						
Damara Belt	NE214	44	1.72	B09	41.8	1.71			
				B10	39.9	1.82			
				B11	44.3	1.72			
				B17	38.8	1.77			
	Ghanzi-Chobe Zone	Main	40	1.87	B06	37.5	1.88		
				(Maun)					
		NE205	38	1.81	B07	40.5	1.95		
		NE206	38	1.69	B08	37.8	1.88		
		NE210	46	1.81	B15	34	1.81		
	NE215	34	1.74						
Passarge Basin	NE209	37	1.84	B05	40.7	1.76			
Nosop Basin	NE203	42	1.76						

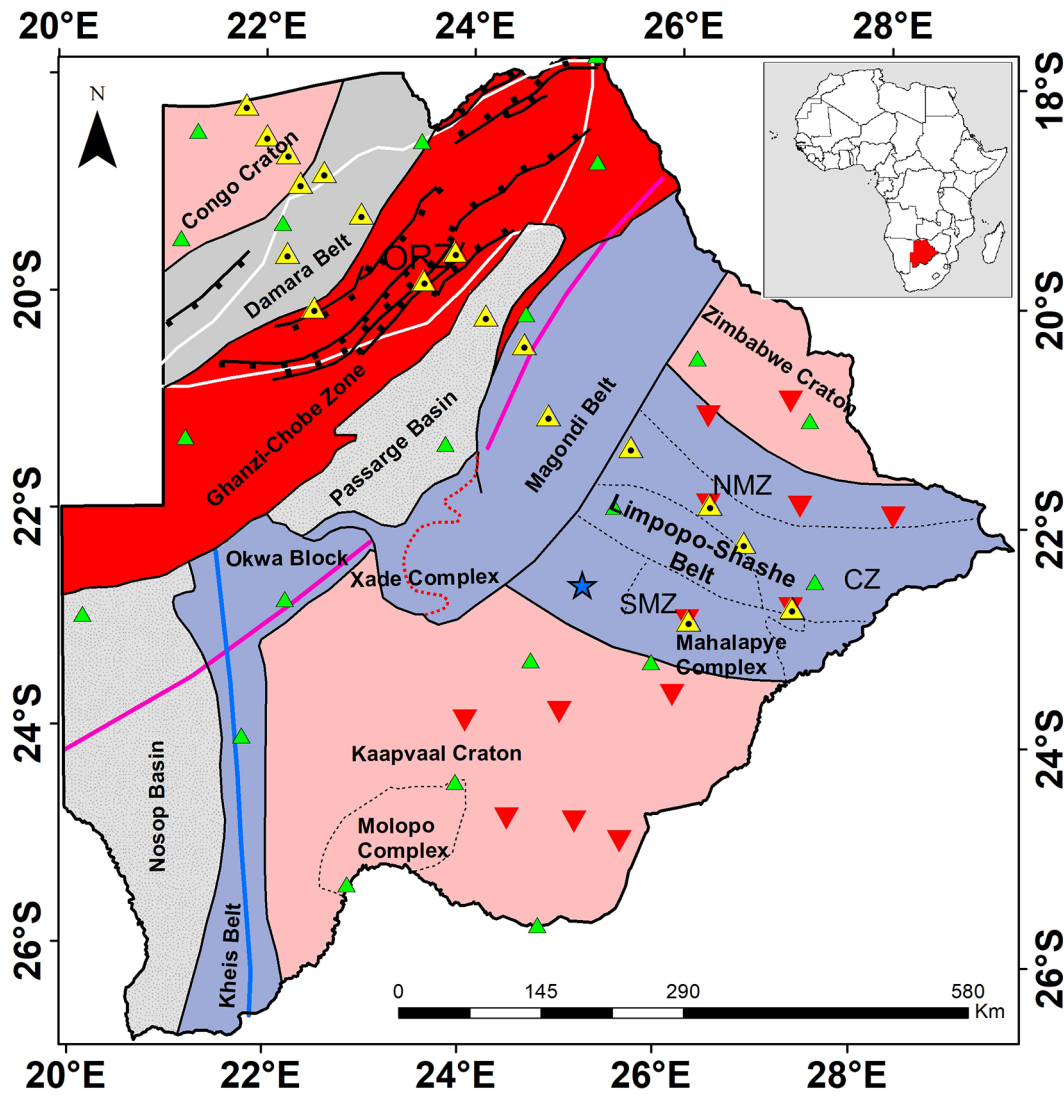
Age	Terrane	This stud y	Tugum e et al. (2013)	Begg et al. (2009)	Kachingw e et al. (2015)	Fadel et al. (2018)	Yu et al. (2015a)	Youssou f et al. (2013)
Archean	Kaapvaal	38 – 45	39	40	39	36 – 42		41 – 46
Crust	Congo	39 - 46	45	39	45	38	46	
	Zimbabw e	39 – 45	36		37	40 – 49	44	39.5 – 50.5
Neo- Archean	Limpopo- Shashe	40 – 46	38		41			41 – 42
Crust								
Proterozoic	Magondi	38 –		39		37 - 40	42	
Crust	Belt	44						
	Ghanzi-	35 –				34 –	37 – 43	
	Chobe	46				46		
	Group							
	Kheis Belt	37 – 41	39	41	43	39		43.5
	Damara Belt	35 44		39	42	44	34 – 44	
	Okwa	38 – 45	43		43	44		
	Block							
Sedimentar y Basin	Passarge	35 – 43				37		
	Nosop	35 – 42		40		42		

<b>Activity</b>	<b>Individuals</b>
Project leader	Mark Van der Meijde
Supervision	Mark van der Meijde, Yan JianGuo
Data provision	Botswana Geoscience Institute through Mark Van Der Meijde
Processing	Chikondi Chisenga
Paper drafting	Chikondi Chisenga
Analysis	Chikondi Chisenga, Mark Van Der Meidje, Yan Jianguo, Islam Fadel, Estella Atekwana, Rabbeca Steffen
discussion	Chikondi Chisenga, Mark Van Der Meidje, Yan Jianguo, Islam Fadel, Estella Atekwana, Rabbeca Steffen
Editing	Chikondi Chisenga, Mark Van Der Meidje, Yan Jianguo, Islam Fadel, Estella Atekwana, Rabbeca Steffen, Calistus Ramotoroko
revising	Chikondi Chisenga, Mark Van Der Meidje, Yan Jianguo, Islam Fadel, Estella Atekwana, Rabbeca Steffen

I would like to ask you to consider our manuscript for publication as a Research Paper in **TECTONOPHYSICS**. I also hereby write to confirm that the paper “**Gravity Derived Crustal Thickness Model of Botswana and its implication to the M<sub>w</sub> 6.5 April 3, 2017, Botswana Earthquake**” is a research paper/letter done as part of a PhD programme in geodesy for Mr Chikondi Chisenga at the State Key Laboratory of Information Engineering in Mapping, Surveying and Remote Sensing of the Wuhan University. Mr Chikondi Chisenga works at the Malawi University of Science and Technology as a Lecturer in Earth Sciences.

The work was made possible by the scholarship offered to Mr Chikondi Chisenga by the Chinese Scholarship Council (CSC). This research was supported by a grant provided by Netherlands Organization for Scientific Research (NWO), grant number A1W-GO-AO/11-30, National Scientific Foundation of China (Grant No. U1831132 and 41274024) and Innovation Group of Natural Fund of Hubei province (Grant No. 2018CFA057). The gravity data was provided by the Geosciences Institute of Botswana, formerly called Geological Survey of Botswana.

- First nationwide gravity derived crustal thickness model for Botswana
- The Congo Craton boundary based on crustal structure in northwestern Botswana is presented for the first time from gravity data
- A proposed causative mechanism for the April 3, 2017  $6.5\text{ M}_w$  Botswana earthquake



#### Moho depth source

- Yu et al. (2015)
- Fadel et al. (2018)
- Youssouf et al. (2013)

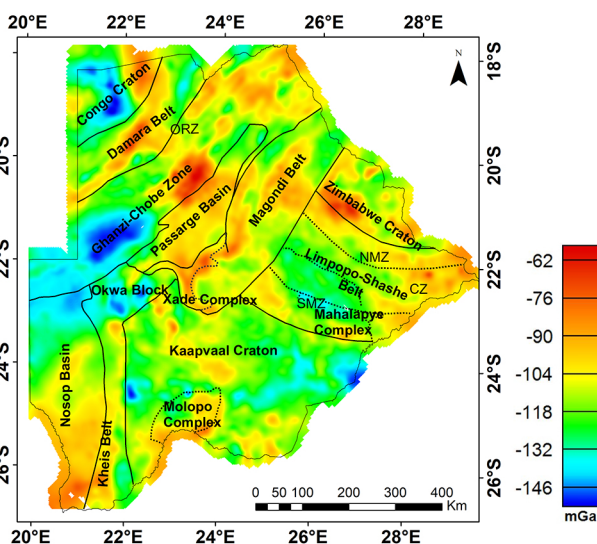
#### Kalahari Suture Zone

- Makgadikgadi Line
- Kalahari Line
- Normal Faults of ORZ
- Xade complex boundary

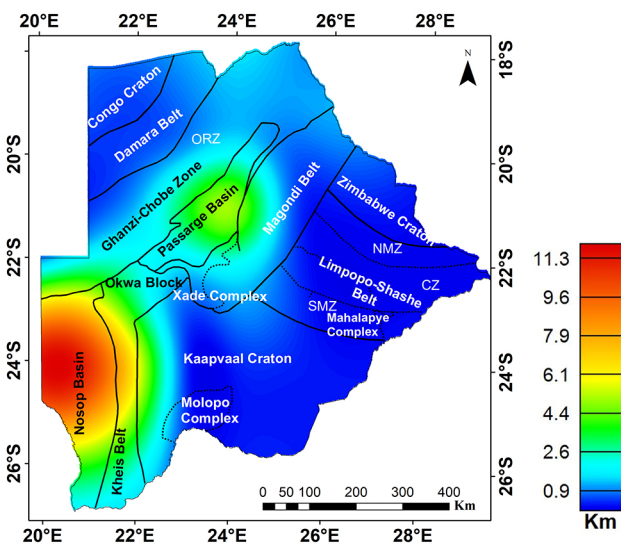
- Paleoproterozoic Orogenic Belt
- Paleo-Mesoproterozoic Orogenic Belt
- Neoproterozoic Orogenic Belt
- Archean Craton
- Sedimentary Basin

Figure 1

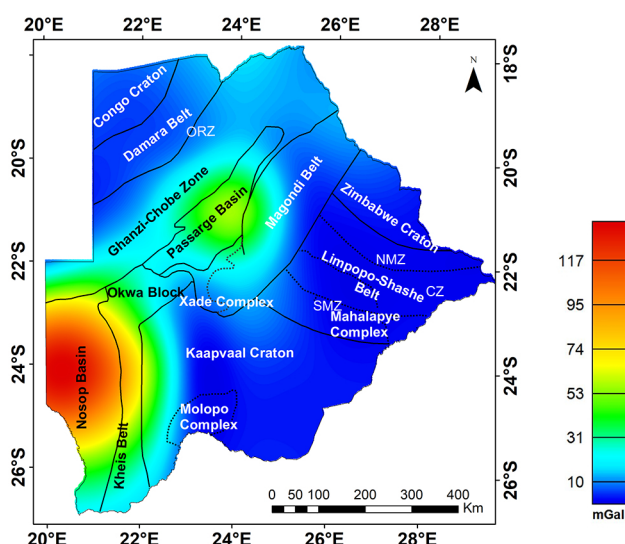
(A)



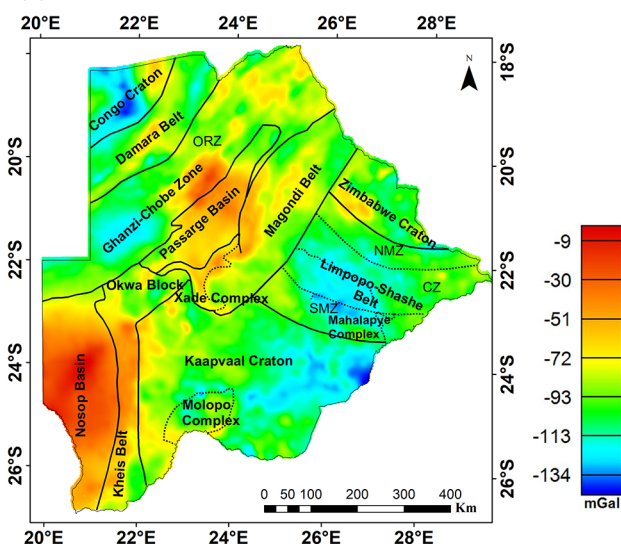
(B)



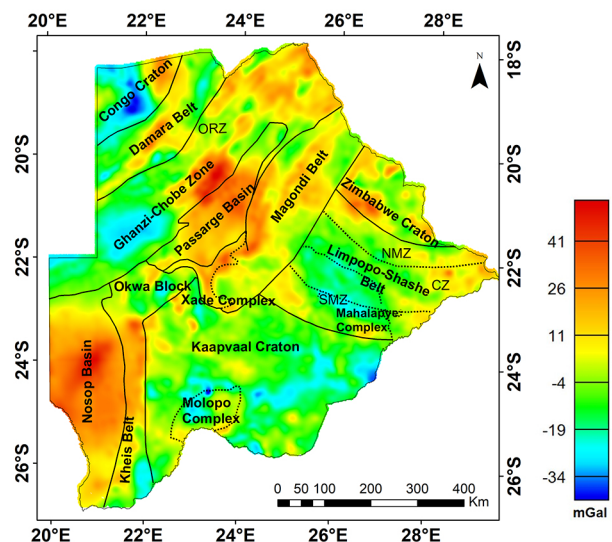
(C)



(D)



(E)



(F)

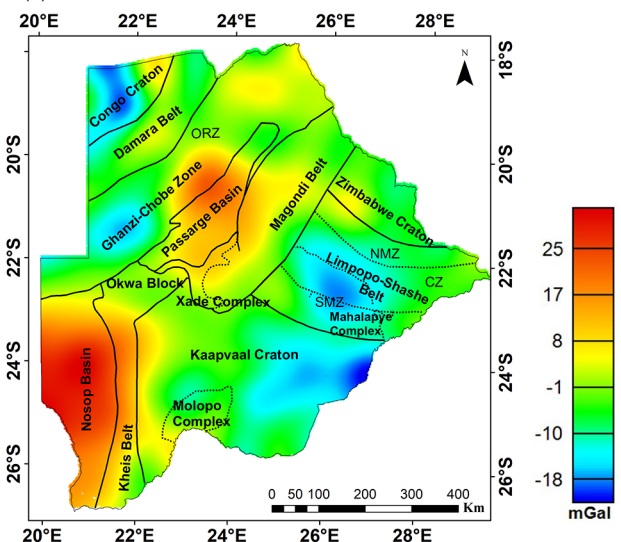


Figure 2

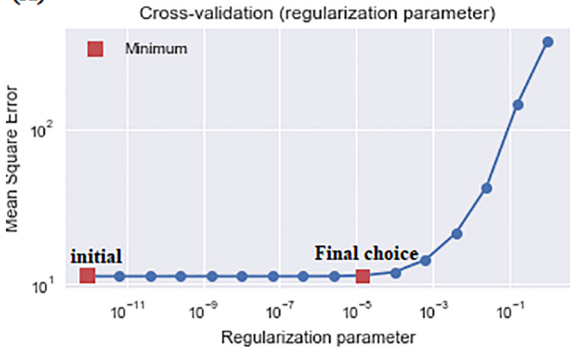
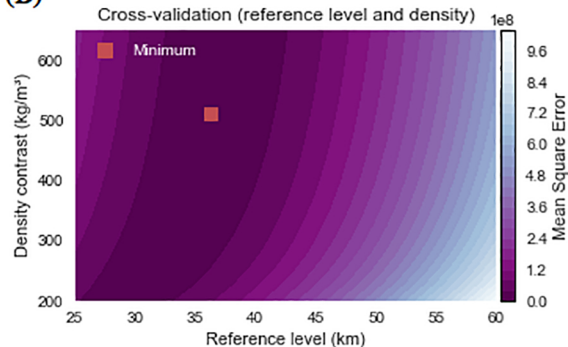
**(A)****(B)**

Figure 3

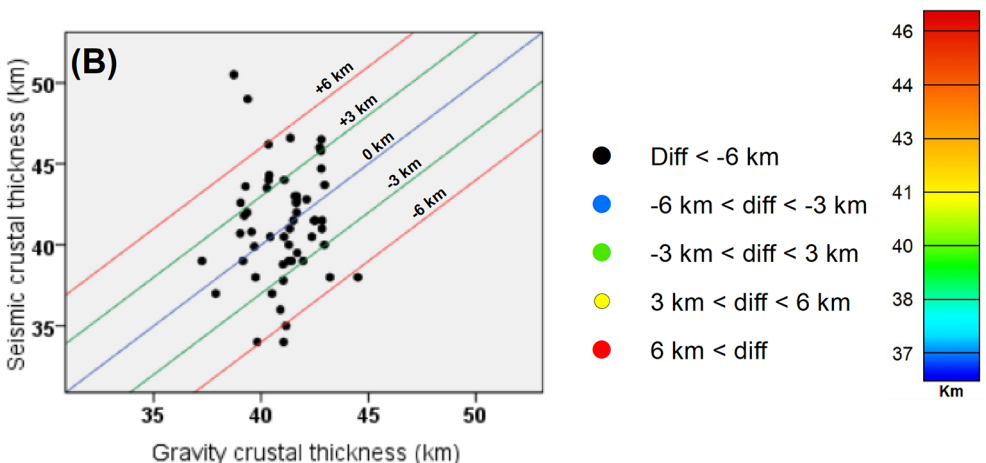
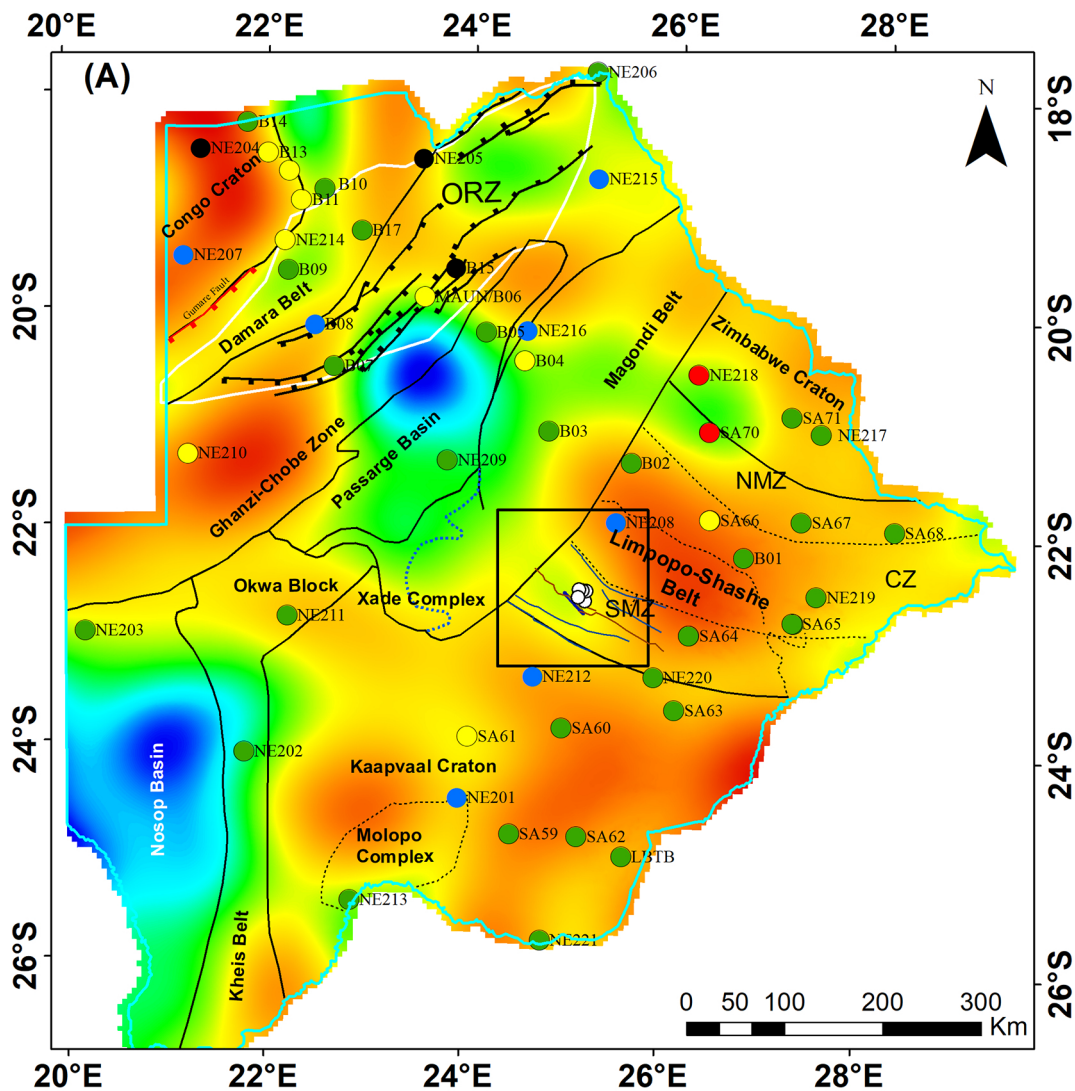
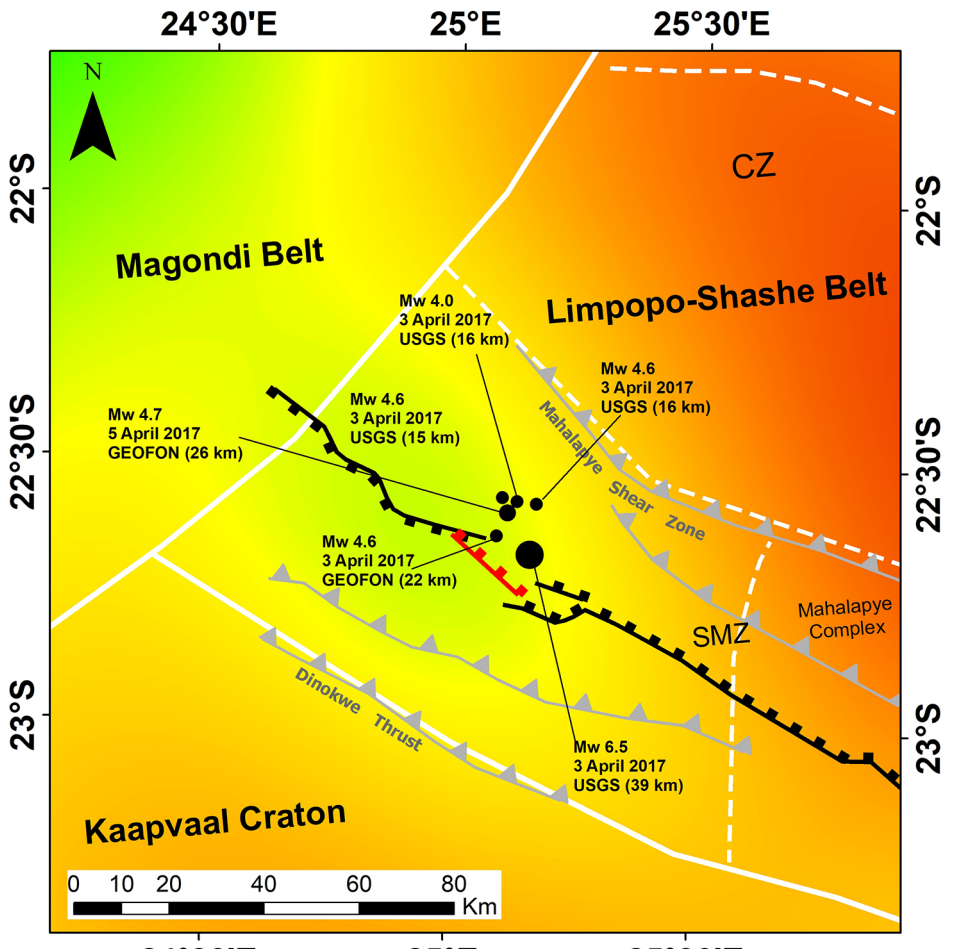


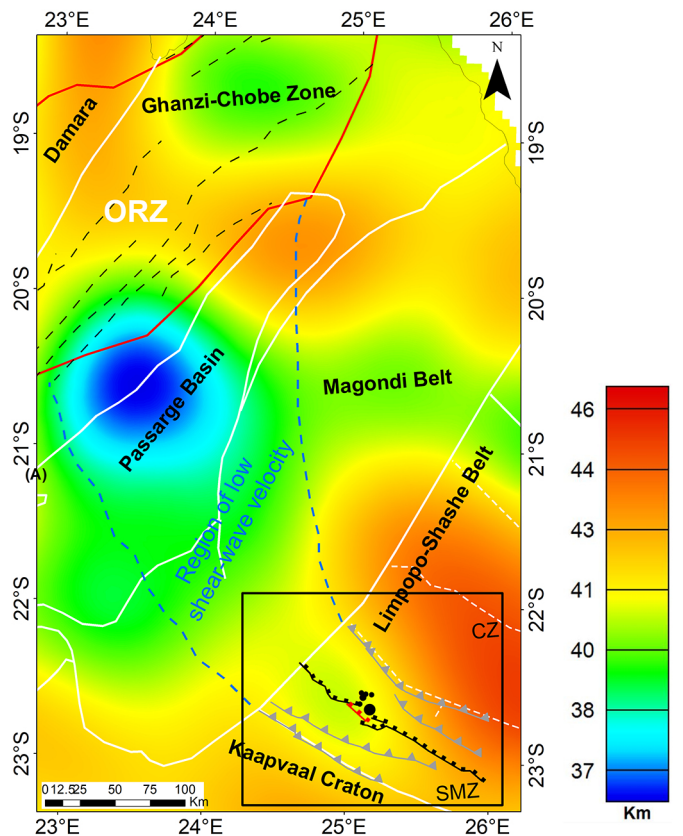
Figure 4



- ▶ Paleoproterozoic thrust fault interpreted from aeromagnetic and gravity data
- ▶ Fault trace from InSAR
- ─ Deep basement fault interpreted from aeromagnetic data
- Main Event
- Main Shock
- After Shock

Figure 5

(A)



(B)

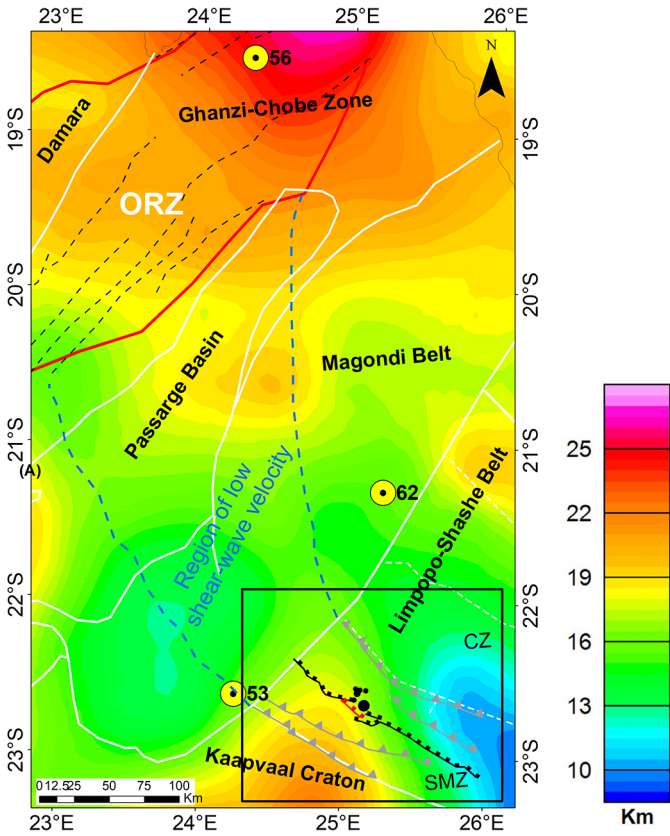


Figure 6